

Fig. 4. Computational complexity of the demodulation for the ML, SDPR-P, and SDPR-D detectors.

where K is the number of users. In effect, the computational complexity for the ML detector increases exponentially with the number of users, whereas that of the SDPR detectors is of polynomial order.

It should be mentioned here that the computational effort pertaining to the SDPR-D detector can be further reduced by taking the special structure of matrix A_i into consideration, but this possibility has yet to be explored.

VI. CONCLUSION

A multiuser detector for DS-CDMA systems based on SDP has been proposed. It has been shown that the ML detection can be carried out by “relaxing” the associated integer programming problem to a dual SDP problem, which leads to a detector of polynomial complexity. Computer simulations that demonstrate that the proposed detector offers near-optimal performance with considerably reduced computational complexity, compared with that of existing primal SDP relaxation-based detectors, have been presented.

REFERENCES

- [1] S. Verdú, “Minimum probability of error for asynchronous Gaussian multiple-access channels,” *IEEE Trans. Inform. Theory*, vol. IT-32, pp. 85–96, Jan. 1986.
- [2] —, *Multiuser Detection*. Cambridge, U.K.: Cambridge Univ. Press, 1998.
- [3] T. Kailath and H. V. Poor, “Detection of stochastic processes,” *IEEE Trans. Inform. Theory*, vol. 44, pp. 2230–2259, Oct. 1998.
- [4] X. M. Wang, W.-S. Lu, and A. Antoniou, “A near-optimal multiuser detector for CDMA channels using semidefinite programming relaxation,” in *Proc. ISCAS*, vol. 4, May 2001, pp. 298–301.
- [5] W.-K. Ma, T. N. Davidson, K. M. Wong, Z. Q. Luo, and P. C. Ching, “Efficient quasimaximum-likelihood multiuser detection by semi-definite relaxation,” in *Proc. ICC*, vol. 1, June 2001, pp. 6–10.
- [6] H. T. Peng and L. K. Rasmussen, “The application of semidefinite programming for detection in CDMA,” *IEEE J. Select. Areas Commun.*, vol. 19, pp. 1442–1449, Aug. 2001.

- [7] L. Vandenberghe and S. Boyd, “Semidefinite programming,” *SIAM Rev.*, vol. 38, pp. 49–95, 1996.
- [8] K. C. Toh, M. J. Todd, and R. H. Tütüncü, SDPT3 Version 2.1—A MATLAB Software for Semidefinite Programming, Sept. 1999.
- [9] P. Gahinet, A. Nemirovski, A. J. Laub, and M. Chilali, *Manual of LMI Control Toolbox*. Natick, MA: MathWorks Inc., May 1990.
- [10] H. Wolkowicz, R. Saigal, and L. Vandenberghe, Eds., *Handbook on Semidefinite Programming*. Hingham, MA: Kluwer, 2000.
- [11] M. X. Geomans and D. P. Williamson, “Improved approximation algorithms for maximum cut and satisfiability problem using semidefinite programming,” *J. ACM*, vol. 42, pp. 1115–1145, 1995.
- [12] —, “.878-approximation algorithms for MAX-CUT and MAX-2SAT,” in *Proc. 26th ACM Symp. Theory Comput.*, 1994, pp. 422–431.
- [13] R. A. Horn and C. R. Johnson, *Matrix Analysis*. Cambridge, U.K.: Cambridge Univ. Press, 1990.
- [14] C. Helmberg, *Semidefinite Programming for Combinatorial Optimization*, Berlin, Germany: Konrad-Zuse-Zentrum, Oct. 2000.
- [15] A. Nemirovskii and P. Gahinet, “The projective method for solving linear matrix inequalities,” *Math. Programming Series B*, vol. 77, pp. 163–190, 1997.
- [16] R. Lupas and S. Verdú, “Linear multiuser detectors for synchronous code-division multiple-access channels,” *IEEE Trans. Inform. Theory*, vol. 35, pp. 123–136, Jan. 1989.
- [17] H. V. Poor and S. Verdú, “Probability of error in MMSE multiuser detection,” *IEEE Trans. Inform. Theory*, vol. 43, pp. 858–871, May 1997.

OFDM Transmitters: Analog Representation and DFT-Based Implementation

Yuan-Pei Lin and See-May Phoong

Abstract—The implementation of OFDM transmitters typically consists of a discrete DFT matrix and a digital-to-analog (DAC) converter. Many existing results on the analysis of OFDM systems, e.g., spectral roll-off, are based on a convenient analog representation. In this paper, we show that the analog representation and the DFT-based OFDM transmitters are equivalent only in special cases. Using the analog system to analyze the DFT-based OFDM system may not be valid if there is no equivalent analog representation.

Index Terms—Analog representation, DFT-based implementation, OFDM, pulse shaping, window.

I. INTRODUCTION

The orthogonal frequency division multiplexing (OFDM) systems [1]–[3] are well known for applications in wireless local area networks (LANs) and broadcast of digital audio and digital video. Fig. 1 shows the schematic of an analog OFDM transmitter with M subcarriers. Let-

Manuscript received November 10, 2002; revised February 20, 2003. The work was supported in parts by the NSC under Grants 90-2213-E-009-108 and 90-2213-E-002-097, by the Ministry of Education, under Contract 89-E-FA06-2-4, Taiwan, R.O.C., and the Lee and MTI Center for Networking Research. The associate editor coordinating the review of this paper and approving it for publication was Dr. Naofal M. W. Al-Dhahir.

Y.-P. Lin is with the Department of Electrical and Control Engineering, National Chiao Tung University, Hsinchu, Taiwan, R.O.C. (e-mail: ypl@cc.nctu.edu.tw).

S.-M. Phoong is with the Department of Electrical Engineering and the Graduate Institute of Communication Engineering, National Taiwan University, Taipei, Taiwan, R.O.C.

Digital Object Identifier 10.1109/TSP.2003.815392

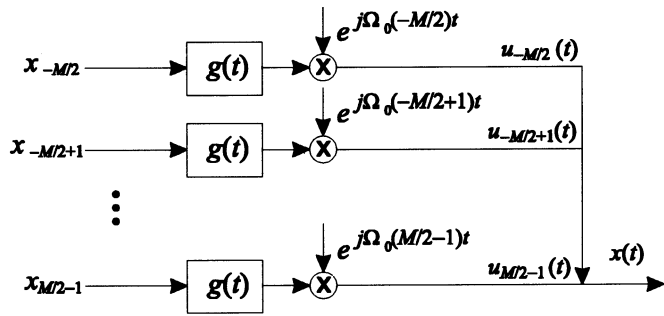


Fig. 1. Baseband analog representation of the OFDM transmitter with M subcarriers and pulse shaping filter $g(t)$.

ting the subcarrier spacing be Ω_0 , the output of the transmitter is given by

$$x(t) = \sum_{k=-M/2}^{M/2-1} x_k g(t) e^{jk\Omega_0 t} \quad (1)$$

assuming M is even. The pulse-shaping filter $g(t)$ is usually a rectangular pulse of length $T_0 = 2\pi/\Omega_0$. Many studies on OFDM systems are carried out using the expression in (1), e.g., the spectral roll-off of the outputs of OFDM transmitters [3], [4], the effect of carrier frequency offset [5], and crest factors of the transmitter outputs [6]. A number of nonrectangular pulse shapes $g(t)$ has been proposed to improve the spectral rolloff of the transmitted signal $x(t)$, e.g., [4] and [6]. Although the analog representation is convenient for analysis, in practice, the modulation of subcarriers is done in the discrete time. Such a transmitter (see Fig. 2) consists of two parts [3]: a digital to analog converter (DAC) and the part performing digital modulation of subcarriers, which can be efficiently implemented using an M by M inverse discrete Fourier transform (IDFT) matrix. The sampling period is $T_s = T_0/M$, and the discrete sequence $w[n]$ shown in Fig. 2 is typically a rectangular window of length M .

Suppose the reconstruction filter of the DAC is $h(t)$, as indicated in Fig. 2. The output of the DAC with sampling period T_s is given by

$$y(t) = \sum_{n=-\infty}^{\infty} y[n] h(t - nT_s) \quad (2)$$

where $y[n] = w[n] \sum_{k=-M/2}^{M/2-1} x_k e^{j(2\pi/M)kn}$.

As indicated in Fig. 2, $y[n]$ is the input of the DAC. The waveform of $y(t)$ resembles that of $x(t)$ —the output of the analog transmitter—especially for large M , [1]. In [3, Ch. 5], it is mentioned that when we use the digital implementation with an ideal lowpass reconstruction filter $h(t)$ in the DAC converter, the shaping filter $g(t)$ is no longer the rectangular pulse. A precise connection between the DFT-based transmitter and the analog representation has not been stated earlier in the literature.

In this paper, we consider the conditions when the DFT-based transmitter in Fig. 2 admits an analog representation in Fig. 1. For the case of a DFT-based transmitter with a rectangular window $w[n]$ and an ideal lowpass $h(t)$, no analog representation exists. It is known that if we choose a rectangular window $g(t)$ in the analog representation, the output is close to that of the DFT-based transmitter in the time domain window, but the two transmitter outputs can have considerable difference in spectral roll-offs. We will show that in fact, when the analog transmitter has a rectangular $g(t)$, a DFT-based implementation does not exist, regardless of the choices of $w[n]$ and $h(t)$. Given an arbitrary pulse $g(t)$, an equivalent digital implementation does not exist in

general. The analog and DFT-based transmitters are equivalent only in some restricted cases. Therefore, analyses of OFDM systems directly using the DFT-based schematic in Fig. 2 are more useful than using the analog schematic in Fig. 1. For example, designing $w[n]$ and $h(t)$ to improve a spectral roll-off is more useful than designing $g(t)$. A necessary and sufficient condition for the equivalence of the analog and DFT-based transmitters will be derived. An example of a set of $g(t)$, $w[n]$, and $h(t)$ that satisfies the condition will be given.

II. ANALOG VERSUS DFT-BASED TRANSMITTERS

Consider the DFT-based implementation of an OFDM transmitter in Fig. 2. Given a discrete window $w[n]$ and a reconstruction filter $h(t)$, we will see that there may not exist a corresponding pulse $g(t)$. For the commonly used case of a rectangular window $w[n]$ and an ideal lowpass $h(t)$, it is mentioned in [3] that the equivalent shaping filter $g(t)$ is not the rectangular pulse. In fact, as we will show in the following lemma, in this case, there does not exist a corresponding analog pulse $g(t)$ at all; it is not possible to analyze the DFT-based transmitter using an equivalent analog transmitter.

Lemma 1: Let the OFDM transmitter in Fig. 2 have a rectangular window $w[n]$

$$w[n] = \begin{cases} 1, & 0 \leq n \leq M-1 \\ 0, & \text{otherwise} \end{cases} \quad (3)$$

and an ideal lowpass reconstruction filter $h(t)$ with

$$H(j\Omega) = \begin{cases} 1, & |\Omega| < \pi/T_s \\ 0, & \text{otherwise.} \end{cases} \quad (4)$$

The outputs of the two systems, respectively, $x(t)$ and $y(t)$, are not the same for any choice of pulse shaping filter $g(t)$.

Proof: Using (2) and the fact that $w[n]$ is as in (3), we arrive at

$$y(t) = \sum_{k=-M/2}^{M/2-1} x_k \sum_{n=0}^{M-1} e^{j(2\pi/M)kn} h(t - nT_s).$$

Comparing this expression with (1), we conclude that $x(t)$ and $y(t)$ are equal for an arbitrary sequence x_k if and only if there exists $g(t)$ such that

$$g(t) e^{jk\Omega_0 t} = \sum_{n=0}^{M-1} e^{j(2\pi/M)kn} h(t - nT_s) \quad (5)$$

for $k = -M/2, -M/2 + 1, \dots, M/2 - 1$.

In particular, the above equation is true for $k = 0$ and $k = 1$. When $k = 0$, we have

$$g(t) = \sum_{n=0}^{M-1} h(t - nT_s).$$

When $k = 1$, we have $g(t) e^{j\Omega_0 t} = \sum_{n=0}^{M-1} e^{j2\pi n/M} h(t - nT_s)$. Let $f(t) = e^{-j\Omega_0 t} h(t)$. Using $\Omega_0 = 2\pi/(MT_s)$, we can rewrite the condition as $g(t) = \sum_{n=0}^{M-1} f(t - nT_s)$. We can verify that $\sum_{n=0}^{M-1} h(t - nT_s) \neq \sum_{n=0}^{M-1} f(t - nT_s)$ and the solution of $g(t)$ obtained for $k = 1$ contradicts the solution of $g(t)$ obtained for $k = 0$. Therefore, (5) cannot be satisfied for any pulse $g(t)$. $\triangle\triangle\triangle$

It is known that the outputs of the analog and DFT-based transmitters are close with proper choices of $g(t)$, $w[n]$ and $h(t)$ [1], [3]. In particular, consider the case that $g(t)$ is a rectangular pulse

$$g(t) = \begin{cases} 1, & 0 \leq t < T_0 \\ 0, & \text{otherwise} \end{cases} \quad \text{where } T_0 = 2\pi/\Omega_0. \quad (6)$$

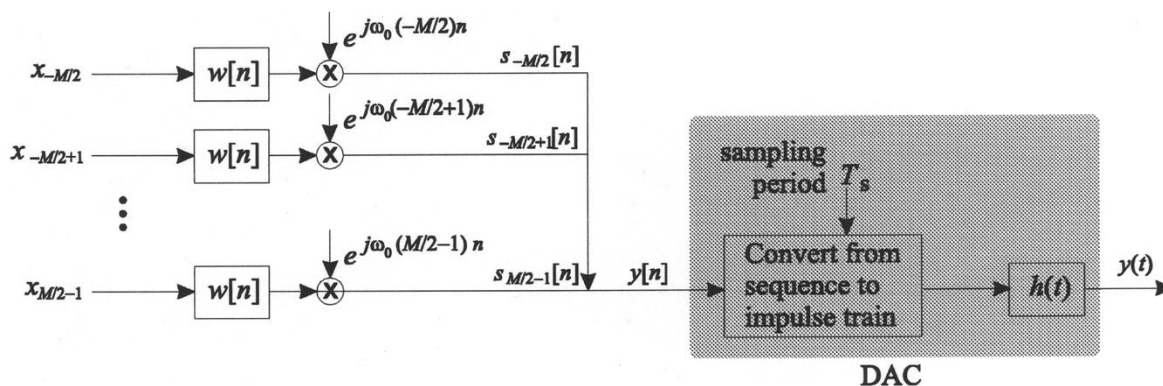


Fig. 2. Commonly used digital implementation of the OFDM transmitter, where $\omega_0 = 2\pi/M$.

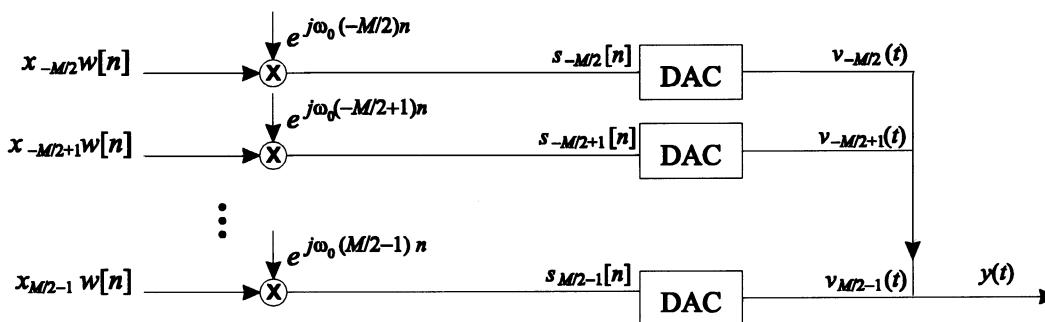


Fig. 3. Equivalent block diagram of system in Fig. 2, where $\omega_0 = 2\pi/M$.

The discrete window $w[n]$ is also rectangular, as given in (3). Choose $h(t)$ to be the ideal lowpass filter given in (4). Then, the samples of $x(t)$ and $y(t)$ are identical, i.e.,

$$x(nT_s) = y(nT_s) = y[n], \quad \text{for all } n. \quad (7)$$

The waveform of $y(t)$ and $x(t)$ are close for the interval $[0, T_0]$, but outside the interval, $x(t)$ comes abruptly to 0, while $y(t)$ has a much smoother transition. Although the energy outside the window is small compared with that inside, this leads to considerably different behaviors between $x(t)$ and $y(t)$ in out-of-band roll-off. We can easily see this by observing that the spectrum of $y(t)$ is bandlimited, whereas the spectrum of $x(t)$ has large sidelobes due to a rectangular $g(t)$. As a result, the analysis of spectral roll-off based on the analog transmitter output $x(t)$ may not be appropriate. To improve spectral sidelobes, designing $w[n]$ and $h(t)$ directly is more meaningful than designing $g(t)$, because $g(t)$ does not allow a DFT-based implementation in general.

Remarks:

- Notice that the relation in (7) does not require $h(t)$ to be an ideal lowpass filter. As long as $h(t)$ satisfies the property $h(nT_s) = \delta[n]$, (7) continues to hold.
- In a DFT-based implementation, typically, a cyclic prefix of length, say L , is added so that ISI can be canceled at the receiver. To this end, we can modify $g(t)$ to be a rectangular window for the interval $[-LT_s, T_0]$. Then, we still have (7).
- In the above derivations, we have used only one OFDM block. If the outputs of the two transmitters are not the same for one block, they will also be different when more blocks are considered.

III. CONDITIONS FOR EQUIVALENCE OF ANALOG REPRESENTATION AND DIGITAL IMPLEMENTATION

We see in the previous section that given a window $w[n]$ and a reconstruction filter $h(t)$, there may not exist a corresponding analog

pulse $g(t)$. Conversely, for a given pulse $g(t)$, a DFT-based implementation does not exist in general. The equivalence of the two systems in Figs. 1 and 2 can be established in certain cases. For the convenience of derivation, we redraw the system in Fig. 2 as Fig. 3, in which the DAC block is as in Fig. 2. The output due to the k -subcarrier is given by $V_k(j\Omega) = S_k(e^{jT_s\Omega})H(j\Omega)$, [9]. Notice that $S_k(e^{j\omega})$ is a frequency-shifted and scaled version of $W(e^{j\omega})$, i.e.,

$$S_k(e^{j\omega}) = x_k W(e^{j(\omega - 2\pi k/M)}).$$

Therefore, we have

$$\begin{aligned} V_k(j\Omega) &= x_k W(e^{j(T_s\Omega - 2\pi k/M)}) H(j\Omega) \\ &= x_k W(e^{jT_s(\Omega - k\Omega_0)}) H(j\Omega) \end{aligned} \quad (8)$$

where we have used the facts that $\Omega_0 = 2\pi/T_0$ and $T_0 = MT_s$. On the other hand, the output of the analog representation in Fig. 1 due to the k th subcarrier is given by

$$U_k(\Omega) = x_k G(j(\Omega - k\Omega_0)).$$

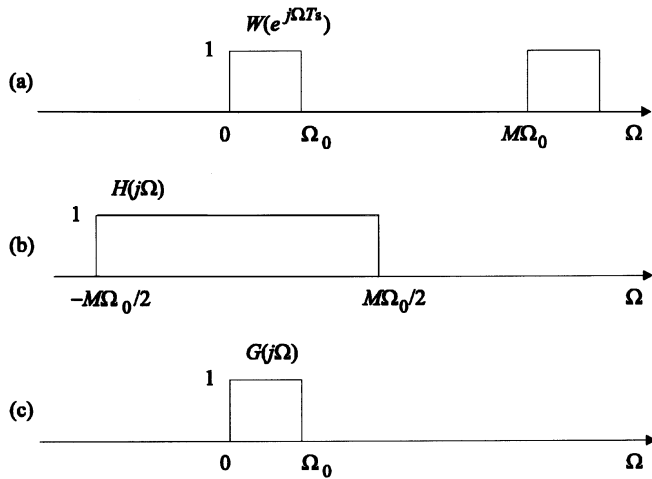
The equivalence of the two systems in Figs. 1 and 2 means that $V_k(\Omega) = U_k(\Omega)$, and therefore

$$W(e^{jT_s(\Omega - k\Omega_0)}) H(j\Omega) = G(j(\Omega - k\Omega_0))$$

for $k = -M/2, -M/2 + 1, \dots, M/2 - 1$. Summarizing, we have the following theorem.

Theorem 1: The OFDM transmitter in Fig. 1 can be implemented as in Fig. 2, namely, the two systems are equivalent, if and only if the pulse shaping filter $g(t)$, the digital window $w[n]$, and the reconstruction filter $h(t)$ satisfy

$$\begin{aligned} W(e^{j\Omega T_s}) H(j(\Omega + k\Omega_0)) \\ = G(j\Omega), \quad \text{for } k = -M/2, -M/2 + 1, \dots, M/2 - 1. \end{aligned} \quad (9)$$


 Fig. 4. Example 1. Illustration of $W(e^{j\Omega T_s})$, $H(j\Omega)$ and $G(j\Omega)$.

In other words, if we are to use a shaping filter $g(t)$ that allows a digital implementation as in Fig. 2, the pulse $g(t)$ should be such that we can find $h(t)$ and $w[n]$ that satisfy (9). Notice that we did not place any constraint on the duration of $g(t)$, $h(t)$, and $w[n]$ in the derivation; the condition in (9) is valid for infinite pulses as well.

Corollary 1: The analog OFDM transmitter with a rectangular pulse $g(t)$ in Fig. 1 does not admit the DFT-based implementation in Fig. 2, regardless of the choices of $w[n]$ and $h(t)$.

Proof: Suppose it admits a digital implementation with $h(t)$ and $w[n]$. Then, by Theorem 2, we have

$$W(e^{j\Omega T_s})H(j(\Omega + k\Omega_0)) = G(j\Omega)$$

where $k = -M/2, -M/2 + 1, \dots, M/2 - 1$
and $G(j\Omega) = e^{-jT_0\Omega/2} \sin(T_0\Omega/2)/\Omega$.

Notice that $G(j\Omega) \neq 0$ for $-\Omega_0 < \Omega < 0$ implies $W(e^{j\Omega T_s}) \neq 0$ for $-\Omega_0 < \Omega < 0$. In turn, this means $H(j\Omega) = H(j(\Omega - M\Omega_0/2))$, for $\Omega \in (-\Omega_0, 0)$. Similarly, the fact that $G(j\Omega) \neq 0$ for $\Omega \in ((-M/2 - 1)\Omega_0, -M/2\Omega_0)$ implies $H(j\Omega) = H(j(\Omega - M\Omega_0/2))$ for $\Omega \in ((-M/2 - 1)\Omega_0, -M/2\Omega_0)$. Combining these two properties of $H(j\Omega)$, we have $H(j\Omega) = H(j(\Omega - M\Omega_0))$, for $-\Omega_0 < \Omega < 0$. Notice that $W(e^{j\Omega T_s})$ is periodic with period $M\Omega_0$ and

$$W(e^{j\Omega T_s})H(j\Omega) = W(e^{jT_s(\Omega - M\Omega_0)})H(j(\Omega - M\Omega_0))$$

for $-\Omega_0 < \Omega < 0$.

This implies $G(j\Omega) = G(j(\Omega - M\Omega_0))$ for $-\Omega_0 < \Omega < 0$, which is not true for a rectangular pulse $g(t)$. $\triangle\triangle\triangle$

An example of $g(t)$, $w[n]$, and $h(t)$ that meet the requirement in (9) is given next.

Example 1: Consider the case where the discrete window $w[n]$ is an ideal filter bandlimited to $0 < \omega < 2\pi/M$ in the period of $0 \leq \omega < 2\pi$. Fig. 4(a) gives a plot of $W(e^{j\Omega T_s})$, which is periodic with period $2\pi/T_s = M\Omega_0$. The reconstruction filter $h(t)$ is an ideal filter of the following frequency characteristics [see Fig. 4(b)]:

$$H(j\Omega) = \begin{cases} 1, & 0 < |\Omega| < M\Omega_0/2 \\ 0, & \text{otherwise.} \end{cases}$$

Choose $g(t)$ to be an ideal filter bandlimited to $0 < \Omega < \Omega_0$, as shown in Fig. 4(c)

$$G(j\Omega) = \begin{cases} 1, & 0 < \Omega < \Omega_0 \\ 0, & \text{otherwise.} \end{cases}$$

We can verify that the condition given in (9) is satisfied and that the analog and the DFT-based transmitters are equivalent. Although there

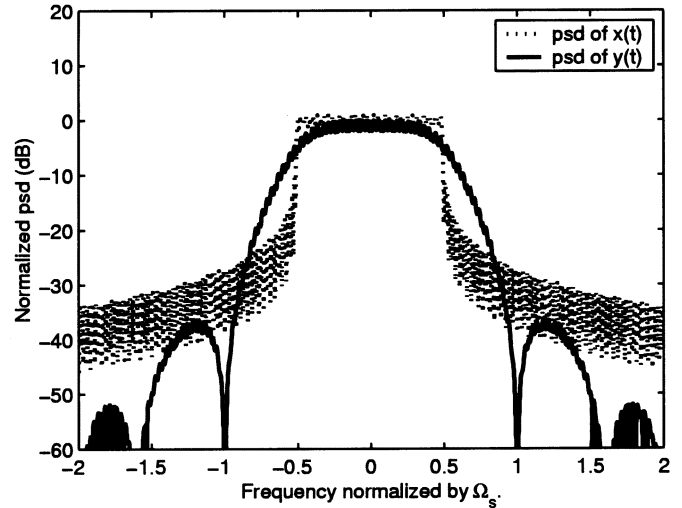


Fig. 5. Example 2. Power spectral densities of the outputs of the two transmitters in Fig. 1 and Fig. 2.

is no practical realization for the functions $g(t)$, $w[n]$, and $h(t)$ in this case, this example demonstrates that the analog representation and DFT-based implementation can be equivalent in some cases.

Example 2: Consider the case $M = 64$. The pulse-shaping filter $g(t)$ for the analog representation in Fig. 1 is a rectangular window, as given in (6). The window $w[n]$ in the DFT-based implementation is a discrete rectangular window as in (3). We choose the reconstruction filter $h(t)$ to be a zero-order hold followed by a second-order elliptical filter. The parameters of the second-order elliptical filter are as follows: Passband ripple size = 1 dB, stopband attenuation = 20 dB, and natural frequency = $0.5 \Omega_s$. Assume that the inputs x_k are uncorrelated modulation symbols with the same variance. The power spectral densities (psd) of the outputs of the two transmitters $x(t)$ and $y(t)$ are as shown in Fig. 5. The maximums have been normalized to one. Notice that for the DFT-based transmitter, the spectrum of the output $y(t)$ depends on the window as well as the reconstruction filter. The spectrum of $x(t)$ and $y(t)$ can be very different, even though rectangular windows are used in both cases.

REFERENCES

- [1] S. B. Weinstein and P. M. Ebert, "Data transmission by frequency-division multiplexing using the discrete Fourier transform," *IEEE Trans. Commun. Technol.*, vol. CT-19, pp. 628–636, Oct. 1971.
- [2] L. J. Cimini, "Analysis and simulation of a digital mobile channel using orthogonal frequency division multiple access," *IEEE Trans. Commun.*, vol. COM-33, pp. 665–675, July 1985.
- [3] G. L. Stuber, *Principles of Mobile Communication*, 2nd ed. Boston, MA: Kluwer, 2001.
- [4] A. Vahlin and N. Holte, "Optimal finite duration pulses for OFDM," *IEEE Trans. Commun.*, vol. 44, pp. 10–14, Jan. 1996.
- [5] T. Pollet, M. Van Bladel, and M. Moeneclaey, "BER sensitivity of OFDM systems to Carrier frequency offset and Wiener phase noise," *IEEE Trans. Commun.*, vol. 43, pp. 191–193, Feb. 1995.
- [6] M. Pauli and P. Kuchenbecker, "On the reduction of the out-of-band radiation of OFDM-signals," in *Proc. IEEE Int. Conf. Commun.*, vol. 3, June 1998, pp. 1304–1308.
- [7] H. Nikoogar and R. Prasad, "Optimal waveform design for multicarrier transmission through a multipath channel," in *Proc. IEEE Veh. Technol. Conf.*, vol. 3, May 1997, pp. 1812–1816.
- [8] K. Matheus and K.-D. Kammeyer, "Optimal design of a multicarrier systems with soft impulse shaping including equalization in time or frequency direction," in *Proc. IEEE Global Telecommun. Conf.*, vol. 1, Nov. 1997, pp. 310–314.
- [9] A. V. Oppenheim, R. W. Schaffer, and J. R. Buck, *Discrete-Time Signal Processing*, 2nd ed. Englewood Cliffs, NJ: Prentice-Hall, 1999.